Future MISFET gate dielectric: NiO/PVA Nanohybride composites

A. Hayati [*]

Department of Science, Faculty of Imam Mohammad Bagher, Mazandaran Branch, Technical and Vocational University (TVU), Mazandaran, I. R. Iran

ARTICLE INFO

ABSTRACT

This paper reports on the electrical and nanostructural properties of polymer-based materials in corporation with NiO (Nickel oxide) in weight concentrations of 0.2%, 0.4%, and 0.8% of PVA (polyvinyl alcohol) polymer. Nanocrystallite phases and properties were characterized by using X-ray diffraction (XRD), Fourier transfer infrared (FTIR) radiation, scanning electron microscopy (SEM), and atomic force microscopy (AFM) techniques. The dielectric constant of the samples has been calculated through measuring the capacity of the samples by application of GPS 132 A. Electrical property characterization was also performed with cyclic-voltameter (C-V) technique in TRIS solution; pH = 7.3, with the formula $(HOCH_2)_3CNH_2$.

1 Introduction

Information technology is resulting from incredibly fast advances in electronics and computing during the last decades. Today the electronics industry is producing metal-oxide-semiconductors (MOS) with very small dimensions [1-4]. The effective oxide thickness of SiO_2 dielectrics in current MOSFET (metal-oxide-semiconductor field effect transistor) is down to 1 nm [5-12]. This size reduction presents challenges for the various SiO_2 applications. As the dimensions of the microelectronic devices are scaled down, the tunneling current of SiO_2 gate dielectric increases exponentially with decreasing the film thickness. For films below 20 Å, the leakage current rises to $1 \sim 10$ A cm^{-2} [5], which is becoming an increasingly critical problem.

Because of the leakage currents due to the quantum tunneling effect, tunneling and light atom penetration through the film that causes performance degradation in electronic materials. Thus, new materials need to be introduced for the next FET devices [13].

Many materials have been investigated to replace silicon dioxide as possible gate dielectrics. Nanomaterials have attracted extensive interest due to their unique properties and aspects, such as catalytic, electronic, and magnetic properties, and incorporation with their bulk counterparts [13]. Nickel oxide (NiO) has demonstrated excellence when being used as a catalyst. Due to the different effects in terms of volume, quantum size, surface, and macroscopic quantum tunnel, nano-sized NiO particles are expected to possess many improved properties over those of bulk and micrometer-sized particles [14-15]. Polyvinyl alcohol (PVA) through their properties has been widely used in various fields. Polyvinyl alcohol has excellent film forming, emulsifying and adhesive properties. It has high tensile strength and flexibility [16-17]. The obtained results indicated that the NiO/PVA with 5 g NiO in weight synthesis at 80 °C

has higher dielectric constant, better morphology, less roughness surface, less leakage current and can be used as a good gate dielectric for the future of OFET (Organic Field Effect Transistor) devices.

2 Experimental

In the present work we have used the sol-gel method for NiO/PVA synthesis. Nickel nitrate hexahydrate $[Ni(NO_3)_2.6H_2O]$ (AR,98%) was used as the metallic precursors for the nanocrystallites, while distilled water was used as solvents nickel nitrate hexahydrate and PVA polymer. 5 g nickel nitrate hexahydrate was dissolved in 50 mL distilled water for 20 min under stirring at 80 °C. 0.6 g sodium hydroxide was added to this solution to adjust the PH value from10-7. On the other container 0.01g PVA (equivalent to 0.2% weight of nickel nitrate hexahydrate) was dissolved in 50 mL water for 20 min under stirring at 80 °C. Then the latter solution was added dropwise to the first and stirred at room temperature. The green resultant sol was stirred continuously for 24 h. Finally, the stabilized sol was changed to gel. The gel was then dried in an oven at 80 ˚C for 24 h where finally a polymeric precursor was gained. Then it was milled and finally powdered. This experiment was also repeated with the same condition for 0.4% and 0.8% PVA. Crystal phases of the nanocrystalites were identified by XRD analysis. Microscopy analysis and surface morphology was performed by using SEM and AFM techniques. Comparison between k values and electrode performance was performed with cyclic-voltameter (C-V) measurements.
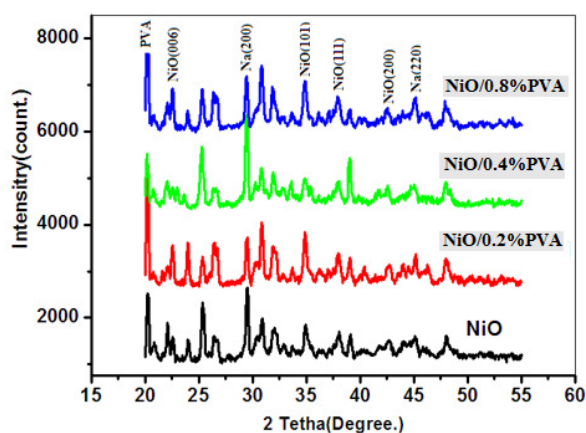

Fig. 1. XRD pattern of NiO and NiO/PVA Nano hybride composite with different content of PVA.

3 Discussion

The crystalline structures and the size of the nanocrystallites were determined by using the XRD technique. In Fig. 1 the spectra XRD pattern (MMA007 (2000)) shows the structure of hexagonal phases β-Ni(OH)$_2$ for the all of the samples.

As the PVA content in the nanocrystallites increased to 0.4%, nanocrystallites polycrystalline phases appear. This indicates that the addition of PVA causes an increase in the degree of crystallinity of the NiO/PVA complex.

The FTIR spectra of the precursor powder dried in 80 °C is illustrated in Fig. 2 in transmittance percentage. Several absorption peaks were observed. The broad absorption band centered at 3550 cm^{-1} was attributable to the O-H bond stretching vibrations, where the band near 1625 cm^{-1} was assigned to H-O-H bending vibration.
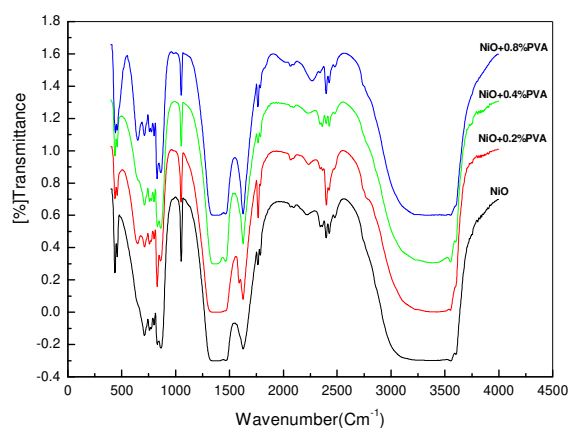

Fig. 2. FTIR spectra of NiO and NiO/PVA Nano hybride composites with different content of PVA.

This provided evidence for the water hydration in the structure, which implies the presence of hydroxyl in the structure. The wide absorption band around 1400 cm^{-1} in the figure indicates the existence of NO$_3$- ions, where the two bands appearing around 600, and 850 cm^{-1} are correlated with the stretching and bending vibrations of the intercalated N-O species in the precursor. This further confirms the presence of NO$_3$- ions. Furthermore, the broad absorption bands appearing around 2250 cm^{-1} in Fig. 1 indicates the existence of CO$_2$ and O=C=O stretching band, which are derived from the powder samples prepared in air. The absorption peaks of Fig. 2 at about 1080 cm^{-1}

belonged to the C-O group. The strong absorption band around 450 cm^{-1} was assigned to Ni-O stretching vibration.

Figure 3 shows EDX analysis obtained from nanocrystallites confirm that the nanocrystallties consists of Ni, Na, O, and C nanoparticles. It is clear that more C content in the composite is obtained with 0.8% PVA.
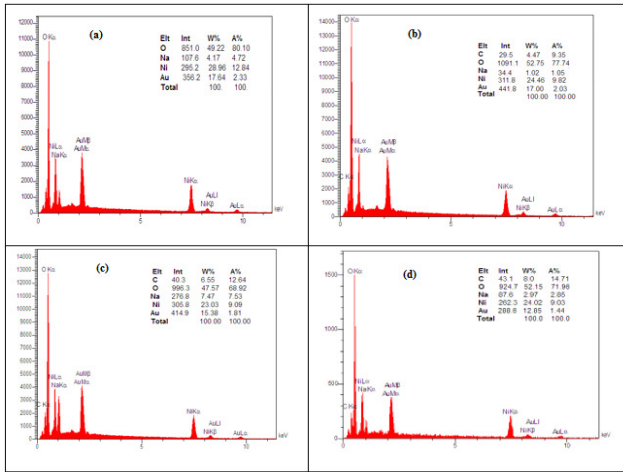

Fig. 3. EDX results for :(a) NiO, (b) NiO/PVA 0.2 wt%, (c) NiO/PVA 0.4 wt%, (d) NiO/PVA 0.8 wt% sample.
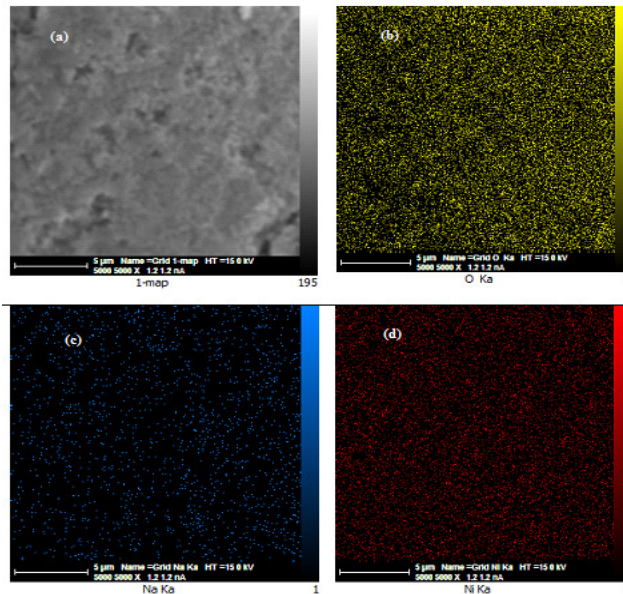

Fig. 4. (a) BSE (Back scanning electron) image and (b,c,d) element map images showing the O, Ni and Na in NiO nanocrystallites.

Furthermore, Fig. 5 shows the elements map images for the NiO/PVA nanostructure. Images, e and f show that carbon nanoparticles are distributed in nickel nanoparticles and almost form a homogenous distribution.
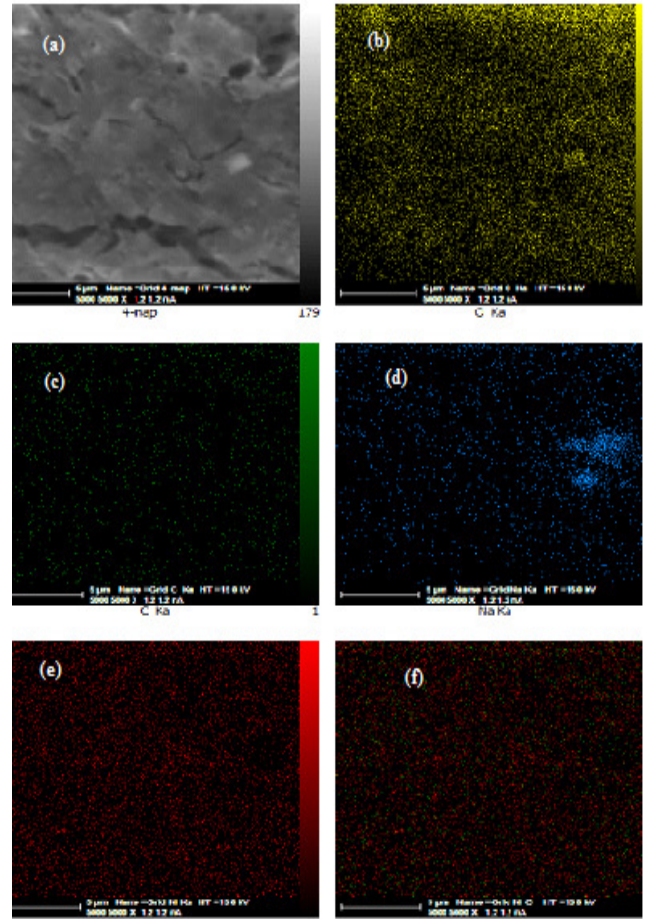

Fig. 5. (a) BSE (Back scanning electron) image and (b,c,d,e) element map images showing the O, C , Na and Ni in NiO+0.8%pva nano hybride composite and (e) element map of combination of NiC.

To study the carrier mobility of nano particles and/or nanocrystallites, we use the DM-SPM technique and analyze the topography spectra from the AFM images (Figs. 6-9).

The tool result section displays the roughness values (the Roughness Average (Sa), mean value (Sm) and the root mean square (Sq)) that are calculated from the data:

$$S_a = \frac{1}{N}\sum_{l=0}^{N-1}\left|z(x_l)\right|,$$

$$S_m = \frac{1}{N}\sum_{l=0}^{N-1}z(x_l), \quad S_q = \sqrt{\frac{1}{N}\sum_{l=0}^{N-1}(z(x_l))^2},$$

The Valley depth, Sv; is the lowest value and the Peak Height, S_p; is highest value. The Peak-Valley Height, is; $S_y = S_p - S_v$.
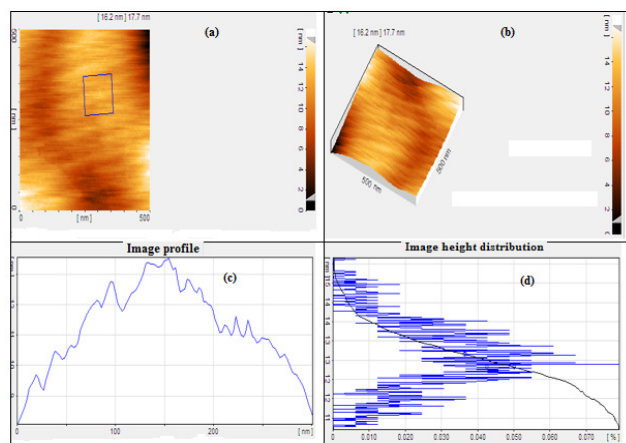

Fig. 6. AFM topography images (2-D) (a) and (3-D) (b) of NiO nanocrystallit and (c,d) diagrams of height distribution of nanoparticles.

Figure 6 exhibits the AFM topographical images of NiO nanocrystallites synthesized at 80 °C. From Table 1 the roughness factor was 1.12 nm and the average roughness of the NiO nanocrystallites synthesized is about 914 pm. The grain size of the nanocrystallites is about 13 nm.

Table.1   roughness factors of NiO, NiO/PVA samples obtained with Nanosurf software.

sample	NiO	NiO/0.2%PVA	NiO/0.4%PVA	NiO/0.8%PVA
S_y	6.45 nm	8.46 nm	5.89 nm	21.0nm
S_z	5.75 nm	7.26 nm	3.72 nm	18.3 nm
S_a	914 pm	1.24 nm	1.03 nm	3.16 nm
S_q	1.12 nm	1.53 nm	1.28 nm	3.93 nm

Figure 7 shows AFM topographical images of NiO+0.2 % PVA nanocrystallites synthesized at 80 °C. From Table 1 the roughness factor was 1.53 nm with the average roughness, S_a, equal to 1.24. The grain size of the NiO/PVA nanocrystallites synthesized is about 5.5 nm. In the AFM image, the island-shaped surface is observed.
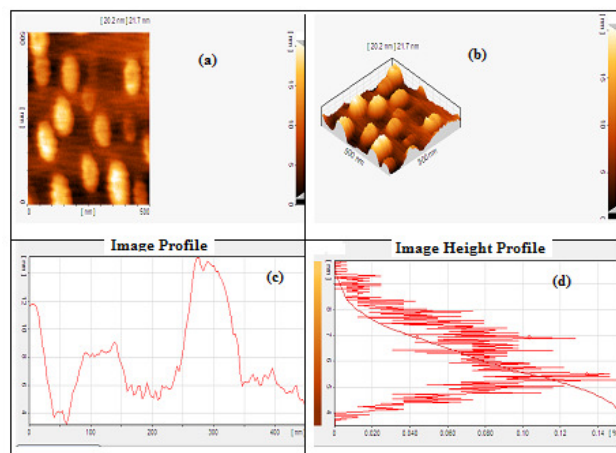

Figure 7. AFM topography images (2-D) (a) and (3-D) (b) of NiO+0.2 % PVA nanocrystallit and (c,d) diagrams of height distribution of nanopartiles.

Moreover from the AFM topographical image (Fig. 8) of NiO+0.4%PVA, the nanocrystallites synthesized at 80 °C, and the data of Table 1, we see that the roughness factor is 1.28 nm and the average roughness, S_a, of the NiO/PVA nanocrystallites synthesized is about 1.03 nm. The grain size of the nanocrystallites is about 7.5 nm.

Fig. 8. AFM topography images (2-D) (a) and (3-D) (b) of NiO+0.4 % PVA nanocrystallit and (c,d) diagrams of height distribution of nanopartiles.

Figure 9 reveals the AFM topographical images of NiO+0.8% PVA nanocrystallites synthesized at 80 °C. The roughness factor was 3.39 nm and the average roughness, S_a, of the NiO/PVA nanocrystallites synthesized is about 3.16 nm. The grain size of the nanocrystallites is about 9 nm.
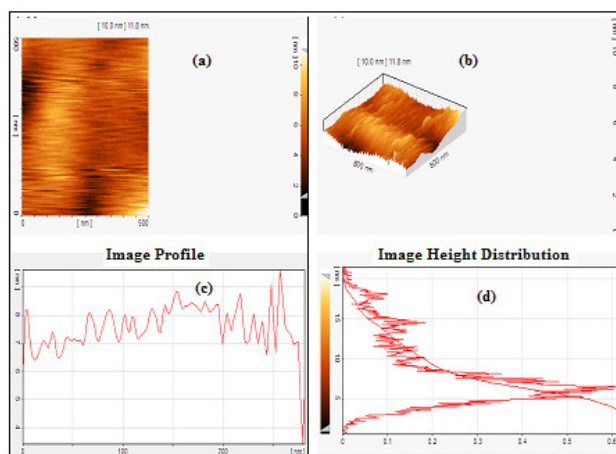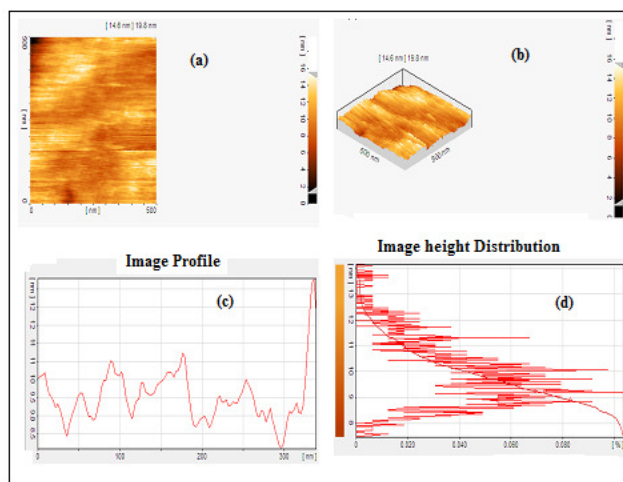
Figure 9. AFM topography images (2-D) (a) and (3-D) (b) of NiO+0.8 % PVA nanocrystallit and (c,d) diagrams of height distribution of nanopartiles.

Nanocrystallites NiO/PVA, with 0.2% PVA showed rougher surface with many grains, and visible crystallites countours, whereas the other samples, especially NiO+0.4 % PVA, had partly a flat and smooth surface morphology. It is clear that more uniform surface is formed for the hybride nanoccomposite with NiO+0.4%PVA.

The SEM (S-14160, 7000 Hitachi) images of NiO/PVA sample are shown in Fig. 10. In Fig. 10a no recognizable crystal grains are seen, but signs of severe brittle fracture on the worn surface are showed. In Fig. 10b some particles are agglomerated. In Fig. 10c, nanocrystallites form a smooth surface. This image reveals an amorphous or quasi amorphous structure that agrees with the XRD spectra of NiO/PVA sample. It is worthwhile to notice that the presence of 0.2% PVA in NiO matrix leads to an agglomeration promoting.

Figure 11 shows the I-V curves obtained with the cyclic-voltameter (C-V) technique for NiO/PVA samples, which annealed at 80 °C.

From the I-V curves we didn't find many differences between NiO/PVA samples for all the concentration nanocrystallites annealed. None of the curves follow Ohm's law because their curve is not a straight line. In fact, the curves follow a

nonlinear rule, this non-linearity is due to the electrical impedance of the samples under test conditions.
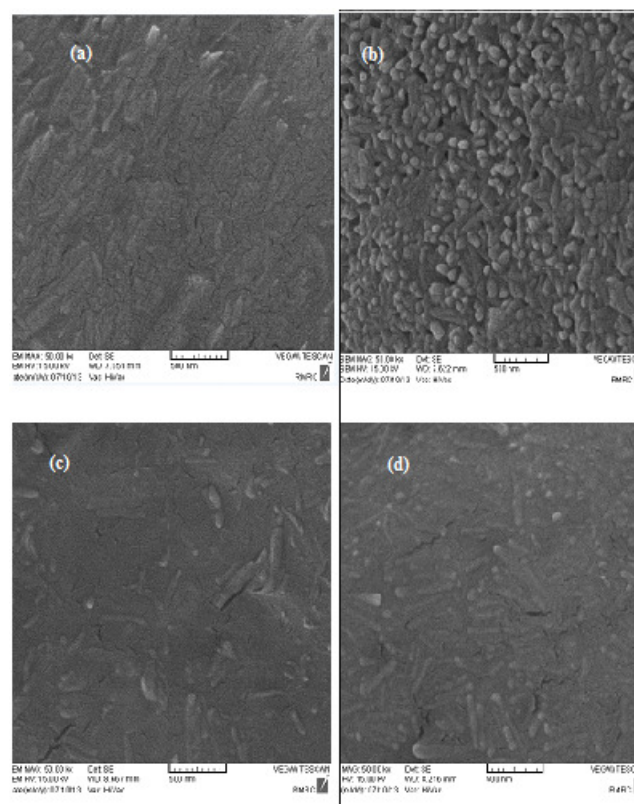

Fig. 10. SEM images of: (a) NiO, (b) NiO+0.2%PVA, (c) NiO+0.4%PVA, (d): NiO+0.8%PVA.
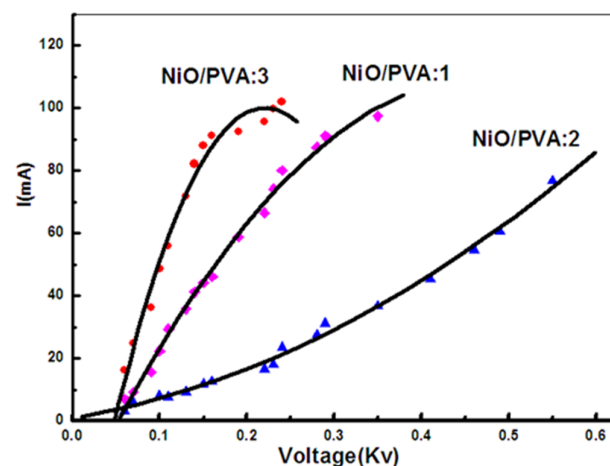

Fig. 11. The I-V curves of NiO/PVA samples

One more point for high percentage of PVA/0.8% is Negative Resistance (NR). Negative Resistance is a property of some electrical circuits and devices in which an increase in voltage across the

device's terminals results in a decrease in the electric current through it. In this case it seems related to Polarons that appear due to increasing PVA of this sample.

By approximation, the graphs 2: NiO / PVA and 3: NiO / PVA are in a certain line of almost linear voltage that can be considered as important contacts. We found the higher dielectric constant for one sample synthesized at 80 ˚C.

The electrical conductivity of NiO//PVA nanocrystallites was also studied at 80 ˚C. The electrical conductivity can be expressed in the simplest form Eq. (1) [18]

$$\sigma = \sigma_0 \exp\left(-\frac{E_a}{kT}\right), \tag{1}$$

where E_a is the activation energy which corresponds to the energy difference between the donor level and the conduction level. σ_0 is a temperature independent factor.

The area under the I-V curves of NiO/PVA nanocrystallites dielectric that has been obtained with the cyclic-voltameter (C-V) technique, is proportional to the power (p = VI). The average value of the current I can be obtained. The optained results presented in Table 2, are the capacitance (C), dielectric constant (K), quality factor (Q_F) and dissipation factor (D_F) for all the samples, where we have

$$P = \int I dv, \tag{2}$$

$$\bar{I} = \frac{P}{\Delta V}. \tag{3}$$

Table 2 C, k, Q_F and D_F of NiO and NiO/PVA obtained with C-V technique, *A=1.13(cm²)*, *Thickness=3(mm)*.

Sample	Q_F	D_F	C(PF)	K
NiO	1.009	0.991	173.5	**52.047**
NiO/0.2%PVA	0.443	2.257	13.7	**41.032**
NiO/0.4%PVA	0.4807	2.08	3.35	**56.48**
NiO/0.8%PVA	0.468	2.136	16.06	**48.173**

Higher Q_F value indicates a lower rate of energy loss with respect to the stored energy of the capacitor as demonstrated in Eq. (5)

$$Q_F = 2\pi \times \frac{Energy\ stored}{energy\ dissipated\ per\ cycle}. \tag{4}$$

The D_F value defined by Eq. (5) gives the loss-rate of energy of the capacitor where it varies with the dielectric material and decreases at higher temperatures as presented in Table 1

$$Q_F = \frac{1}{D_F}. \tag{5}$$

Mathematically, expression for the current density according to Poole-Frenkel model can be written as [19]

$$J = AT^2 exp \frac{1}{kT}\left[\left(\frac{57.7\ eV}{\varepsilon_1 d}\right)^{\frac{1}{2}} - \varphi\right], \tag{6}$$

where ε_l is the dielectric constant of the film, d is electrode spacing in Å , φ is the depth of the trap potential well and A which is the Richardson constant is equal to 120 A/cm² k². The obtained results show that the sample without organic material has maximum value of dielectric constant that could be synthesized.

It is obvious that the I-V trend is a sextic function behavior given by

$$I = aV^6 + bV^5 + cV^4 + dV^3 + fV + g, \tag{7}$$

where the coefficients a, b, c, d, e, f and g are specified in Table 3.

Table 3 Sextic function coefficients for NiO, NiO/PVA

	Function coefficients(×1.0E+4)				
Sample	a	b	c	d	e	f
NiO/0.2%PVA	-1122	852.6	-231.8	30.8	-1.9	0
NiO/0.4%PVA	38304	-19443	3825	-364	17	0
NiO/0.8%PVA	10204	-10143	2541	-328	-2.3	0

4 Conclusions

In the present work, the electrical properties of the NiO/PVA nanocrystallites prepared by the sol-gel method were studied. The XRD analysis revealed that as the PVA content in the nanocrystallites increase, generally the peaks intensity increased and shifted. The Poole-Frenkel effect observed due to the trap levels originated from the defect levels indicate that the adsorbed oxygen atoms present in the grain boundary regions can change the nano structural electrical properties. Since the permittivity value of NiO/PVA dielectric is higher than for other presented samples, therefore it can be introduced as a good gate dielectric material for the next CMOS generation

Acknowledgments

References

[1] P. R. Giri. "Atom Capture by Nanotube and Scaling Anomaly." International J. of Theoretical Physics, **47** (2008) 1776.

[2] Y. J. Lee. "Formation of aluminum nitride thin films as gate dielectrics on Si (1 0 0)." J. Crystal Growth, **266** (2004) 568.

[3] H. Wu, Y. Zhao, M. H. White. "Quantum mechanical modeling of MOSFET gate leakage for high-k gate dielectrics." Solid–State Electron, **50** (2006) 1164.

[4] M. Wu, Y. I. Alivov, H. Morkoc. J. Mater. Mater "High-κ dielectrics and advanced channel concepts for Si MOSFET." J. Materials Science: Materials in Electronics, **19** (2008) 915.

[5] G. D. Wilk, R.M. Wallance, J. M. Anthony. "High-κ gate dielectrics: Current status and materials properties considerations." J. Applied Physics, **89** (2001) 5243.

[6] S. Zafar, A. Kumar, E. Gusev, E. Cartier, "Threshold voltage instabilities in high-/spl kappa/gate dielectric stacks." IEEE Transactions on Device and Materials Reliability, **5** (2008) 45.

[7] M. Zaharescu, V. S. Teodorescu, M. Gartner, M. G. Blanchin, A. Barau, M. Anastasescu. "Correlation between the method of preparation and the properties of the sol–gel HfO2 thin films." J. Non –Crystalline solids, 354 (2008) 409.

[8] A. Deman, L. Tardy. "PMMA–Ta2O5 bilayer gate dielectric for low operating voltage organic FETs." Organic Electronics, 6 (2005) 78.

[9] S. G. Pandali, *New york,* Transworld research network, 2002.

[10] H. J. Liu, Z. X. Xie, H. Watanabe, J. Qu, K. Tanaka. "Growth of nanocrystalline metal dots on the Si(111)-7×7 surface saturated with COH." Physical Review B, **601** (2007) 5093.

[11] W. J. Qi, R. Nieh, B. H. Lee, L. G. Kang, Y. Jeon, K. Onishi, T. Ngai, S. Banerjee and J. C. Lee. "High-κ gate dielectrics: Current status and materials properties considerations." Technical Digest-International Electron Device Meeting, **7** (1999) 145.

[12] N. Gang, Y. Wu, T. Lili, G. Hao, Z. Wenhao, G. Jinzhang. "Preparation of polystyrene/SiO2 nanocomposites by surface-initiated nitroxide-mediated radical poly-merization." Chinese Science Bulletin, **51** (2006) 1644.

[13] M. Alagiri, S. Ponnusamy, C. Muthamizhchelvan. "Synthesis and characterization of NiO nanoparticles by sol–gel method." J. Materials Science: Materials in Electronics, **23** (2012) 728.

[14] A. Hayati and A. Bahari, "Electrical properties of NiO/PVC nano hybrid composites for organic field effect transistors." Indian J. of Physics, **89** (2015) 45.

[15] A. Hayati and A. Bahari, "Synthesis and study of electrical properties of NiO/ PVC nano hybride composites as a gate dielectric material of OFET." Applied Physics (Elzahrah), **2** (2014) 23.

[16] A. Hayati and A. Bahari. "Investigation of Electrical and Optical Characteristics of Nanohybride Composite (Polyvinyl Alcohol / Nickel Oxide)." JNS, **4** (2014) 9.

[17] F. Garnier, R. Hajlaoui, X. Peng, D. Fichou. "An all-organic "soft" thin film transistor with very high carrier mobility." Advanced Materials, **2** (1990) 592.

[18] R. Ponce Ortiz, A. Facchetti and T. J. Marks. "High-k Organic, Inorganic, and Hybrid

Dielectrics for Low-Voltage Organic Field-Effect Transistors." Chemical Reviews, **110** (2010) 205.

[19] X. Peng, G. Horowitz, D. Fichou, F. Garnier. "All-organic thin-film transistors made of alpha-sexithienyl semiconducting and various polymeric insulating layers." Applied Physics Letters, **1990** (2013) 57.